Acta Crystallographica Section F
Structural Biology and Crystallization Communications
ISSN 1744-3091

Purification, crystallization and preliminary X-ray crystallographic analysis of the outer membrane lipoprotein NlpE from *Escherichia coli*

Yu Hirano,[a]‡ Md. Motarab Hossain,[b]‡ Kazuki Takeda,[a,c] Hajime Tokuda[b] and Kunio Miki[a,c]*

[a]Department of Chemistry, Graduate School of Science, Kyoto University, Sakyo-ku, Kyoto 606-8502, Japan, [b]Institute of Molecular and Cellular Biosciences, University of Tokyo, 1-1-1 Yayoi, Bunkyo-ku, Tokyo 113-0032, Japan, and [c]RIKEN SPring-8 Center at Harima Institute, 1-1-1 Koto, Sayo, Hyogo 679-5198, Japan

‡ These authors contributed equally to this work.

Correspondence e-mail: miki@kuchem.kyoto-u.ac.jp

Received 30 September 2006
Accepted 30 October 2006

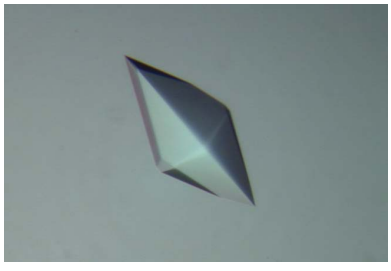

The outer membrane lipoprotein NlpE functions in stress response by activating the Cpx signal transduction pathway. The nonlipidated Cys1Ala mutant of NlpE with a C-terminal His tag from *Escherichia coli* was constructed, overexpressed and purified. Crystals of NlpE were grown in two distinct forms by the sitting-drop vapour-diffusion method at 298 K. The tetragonal crystals diffracted to 2.8 Å resolution and belong to space group $P4_32_12$. The monoclinic crystals diffracted to 3.0 Å resolution and belong to space group $C2$. Initial phases were obtained from a tetragonal crystal of selenomethionylated protein by the MAD method.

1. Introduction

NlpE (new lipoprotein E) from *Escherichia coli* is a 24 kDa lipoprotein possessing three acyl chains at the cysteine residue of position +1 (Snyder *et al.*, 1995). Homologous proteins are widely found in Gram-negative bacteria. The protein is anchored on the periplasmic side of the outer membrane with the acyl chains. The localization is achieved by the Lol proteins (Matsuyama *et al.*, 1995, 1997; Yakushi *et al.*, 2000) owing to the absence of the Lol avoidance signal made up of residues at positions +2 and +3 (Yamaguchi *et al.*, 1988; Terada *et al.*, 2001; Masuda *et al.*, 2002). On the outer membrane, NlpE has been reported to detect envelope stress caused by cell adhesion to hydrophobic surfaces (Otto & Silhavy, 2002). An external copper ion is also thought to be detected by NlpE (Yamamoto & Ishihama, 2005, 2006). These stresses induce the transcription of periplasmic proteins such as the periplasmic protease/chaperone DegP (Danese *et al.*, 1995), the peptidyl-prolyl isomerases PpiA (Pogliano *et al.*, 1997) and PpiD (Dartigalongue & Raina, 1998) and the disulfide oxidase DsbA (Pogliano *et al.*, 1997) through the Cpx pathway. The Cpx pathway, which is one of the two-component signal transduction pathways (Raivio *et al.*, 1999; Raffa & Raivio, 2002; Duguay & Silhavy, 2004; Ruiz & Silhavy, 2005), contains an inner membrane histidine kinase CpxA and a cytoplasmic response regulator CpxR. External stresses induce an autophosphorylation reaction at the cytoplasmic domain of CpxA. After the reaction, the phosphate is transferred from CpxA to CpxR and the phosphorylated CpxR then initiates gene transcription. In addition, a periplasmic protein CpxP has been reported to regulate Cpx signal transduction by binding to the sensor domain of CpxA (Danese & Silhavy, 1998; Raivio *et al.*, 1999, 2000; Buelow & Raivio, 2005; Isaac *et al.*, 2005). However, the molecular mechanism by which NlpE detects the envelope stresses and transmits the signals to the Cpx pathway remains unclear.

Three regions of the amino-acid sequence of NlpE from *E. coli* are responsible for the lipoprotein's function. Firstly, the sequence 31-CADC is suggested to bind divalent cations such as Zn^{2+} and Cu^{2+} or to be involved in redox regulation. Indeed, NlpE has also been identified as the copper homeostasis protein CutF (Gupta *et al.*, 1995). Secondly, the sequence 124-MTPMTLRGMYFYM including four methionines is similar to the copper-binding motif of the copper-trafficking protein CopC, as mentioned previously (Arnesano *et al.*, 2003). Thirdly, the sequence 99-MLDREGNPIESQFNYTL resembles the serine protease inhibitor signature that exists in the N-terminus of inhibitors (Mares *et al.*, 1989). In the crystal structure of soybean trypsin inhibitor complexed with porcine trypsin, the

inhibitor signature is located in the vicinity of the reactive-site loop (Song & Suh, 1998). Therefore, elucidation of the NlpE structure would make a significant contribution to the study of the stress response in the periplasmic space of Gram-negative bacteria. In this paper, we report the construction, purification, crystallization and preliminary X-ray crystallographic analysis of a water-soluble mutant of NlpE from *E. coli*.

2. Materials and methods

2.1. Overexpression and purification

Because the outer membrane lipoprotein NlpE is insoluble, a soluble mutant of NlpE (mNlpE) with a Cys-to-Ala substitution at position +1 was used for crystallization (Fig. 1). While the signal sequence of the mutant is cleaved after secretion to the periplasm, the resulting N-terminal Ala1 is not modified by hydrophobic acyl chains. Construction of a plasmid (pKT-mNlpE) carrying the *mnlpE* gene was performed using a previously reported method (Matsuyama *et al.*, 1997; Miyadai *et al.*, 2004). mNlpE was constructed so as to have a T7 tag followed by a His tag at the C-terminus. Expression plasmids of mNlpE were transformed into *E. coli* K-12 strain MC4100 cells. Cells were grown at 310 K with aeration in Luria–Bertani (LB) broth. The antibiotic ampicillin (50 µg ml^{-1}) was used for the selection of plasmid-containing cells. mNlpE was prepared from the periplasmic fraction using a previously reported method with slight modification (Matsuyama *et al.*, 1995). TALON resin (BD Biosciences, San Jose, CA, USA) was packed into a 10/150 column and then washed with a washing buffer containing 50 m*M* sodium phosphate pH 7.2 and 0.3 *M* sodium chloride. The periplasmic fraction containing mNlpE was applied onto the column and washed with the washing buffer. The binding proteins were eluted with an elution buffer containing 50 m*M* sodium phosphate pH 7.2, 0.3 *M* sodium chloride, 10%(*v*/*v*) glycerol and 250 m*M* imidazole. The eluted proteins were concentrated to less than 50 ml using centrifugal filter devices (Amicon, Danvers, MA, USA). All proteins were further purified by application onto an HA column (Tosoh, Tokyo, Japan) which had been equilibrated with 25 m*M* potassium phosphate pH 7.5, 10%(*v*/*v*) glycerol and 0.01 m*M* calcium chloride. The eluted proteins were transferred to buffer containing 25 m*M* potassium phosphate pH 7.5 and 10%(*v*/*v*) glycerol and concentrated to 35 mg ml^{-1} with an Amicon ultracentrifugal filter device. The purified proteins were analyzed by SDS–PAGE with Coomassie brilliant blue staining. The molecular weight of the purified protein was determined by matrix-assisted laser-desorption ionization mass spectrometry (MALDI–MS) with a Voyager-DE PRO (Applied Biosystems, Foster City, USA). A Sequazyme Peptide Mass Standard Kit (Applied Biosystems) was used for calibration. Sinapinic acid (10 mg ml^{-1}) dissolved in 50%(*v*/*v*) acetonitrile containing 0.1%(*v*/*v*) trifluoroacetic acid was used as a matrix. Samples for MALDI–MS experiments were prepared by mixing 1 µl protein sample and 1 µl matrix solution. 0.5 µl samples was directly loaded on a MALDI target plate.

Selenomethionine-labelled protein was produced in the methionine-auxotrophic *E. coli* strain P4X8 (Hfr P4X λ$^-$ *metB1*) as previously reported (Takeda *et al.*, 2003). Cells were grown at 310 K in minimal medium containing selenomethionine and proteins were purified using the same protocol as for unlabelled mNlpE.

2.2. Crystallization

Crystallization of the unlabelled protein was performed at 298 K by the sitting-drop vapour-diffusion method using 24-well tissue-culture plates. Initial crystallization trials were performed using sparse-matrix kits (Crystal Screen, Crystal Screen 2 and Crystal Screen Cryo; Hampton Research, Laguna Niguel, CA, USA). Clustered crystals were obtained under several conditions containing polyethylene glycol (PEG) 8000. Further optimization of crystallization conditions gave two crystal forms suitable for diffraction experiments by varying the pH, salt and PEG 8000 concentration. Pyramidal crystals (form I) were obtained by mixing 1.0 µl protein solution (35 mg ml^{-1}) with an equal volume of reservoir solution on a microbridge (Hampton Research). The drop was equilibrated against 600 µl reservoir solution containing 14%(*w*/*v*) PEG 8000, 50 m*M* sodium citrate pH 4.0, 160 m*M* zinc sulfate and 40%(*w*/*v*) D-sorbitol. Another crystal form (form II) was obtained by mixing 10 µl protein solution (2.5 mg ml^{-1}) with 1.0 µl reservoir solution. The drop was equilibrated against 600 µl reservoir solution containing 20%(*w*/*v*) PEG 8000, 20 m*M* sodium acetate pH 4.0, 100 m*M* sodium formate and 15%(*v*/*v*) ethylene glycol. Form I crystals of the selenomethionylated protein were obtained in 14%(*w*/*v*) PEG 8000, 50 m*M* sodium citrate pH 4.2, 70 m*M* zinc sulfate and 40%(*w*/*v*) D-sorbitol.

2.3. X-ray diffraction experiment and phase determination

All diffraction data were collected at beamline BL44B2 of SPring-8 using an ADSC Quantum 210 detector (Adachi *et al.*, 2001). Before collecting diffraction data from form I crystals of the unlabelled protein, crystals were transferred into reservoir solution supplemented with 2 m*M* samarium acetate for 15 h. Subsequently, crystals were flash-cooled in a nitrogen-gas stream at 90 K. An annealing protocol was applied in order to improve the diffraction quality (Yeh & Hol, 1998). The wavelength of the incident X-rays was 1.6000 Å and the crystal-to-detector distance was 150 mm. A data set consisting of 180 frames was collected with a rotation angle of 1° and an exposure time of 60 s per frame. The data from form II crystals of the unlabelled protein were collected with an incident X-ray wavelength of 1.0000 Å and a crystal-to-detector distance of 300 mm. A data set consisting of 180 frames was collected with a rotation angle of 1° and an exposure time of 60 s per frame. Multiwavelength anomalous dispersion (MAD) data were collected at four X-ray wavelengths from a selenomethionyl derivative crystal. Peak (0.9792 Å) and edge (0.9797 Å) wavelengths were determined based on the X-ray

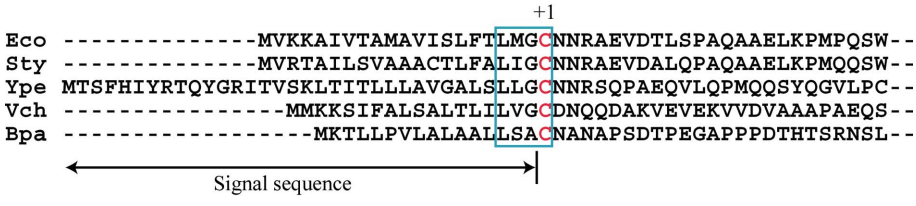

Figure 1
The N-terminal residues (signal sequence and mature region) of NlpE homologues. Cys residues at position +1 are indicated by red characters. The indicator of bacterial lipoprotein (lipobox) is indicated by a cyan box. Eco, *Escherichia coli*; Sty, *Salmonella typhimurium*; Ype, *Yersinia pestis*; Vch, *Vibrio cholerae*; Bpa, *Bordetella parapertussis*.

absorption spectrum. Low-energy and high-energy remote wavelengths were selected at 0.9900 and 0.9700 Å, respectively. The crystal-to-detector distance was 300 mm. Each data set consisting of 180 frames was collected with a rotation angle of 1° and an exposure time of 20 s per frame. All data were processed and scaled using the *HKL*-2000 program package (Otwinowski & Minor, 1997). Pseudo-precession photographs for the determination of screw axes were displayed using *XtalView* (McRee, 1999). The program *SHELXD* was used to determine Se-atom sites (Schneider & Sheldrick, 2002). Phase calculation and subsequent density modification were performed using the program *CNS* (Brünger *et al.*, 1998). Initial electron-density maps were displayed with *XtalView*.

3. Results and discussion

Proteins suitable for crystallization were obtained by cobalt-affinity and gel-filtration chromatography (Fig. 2*a*). The molecular weight of mNlpE was determined to be 24 597 Da by MALDI–MS experiments (Fig. 2*b*), while the calculated molecular weight of mature mNlpE is 25.6 kDa. Therefore, a truncation of a further ten residues may be occurring at the N-terminus. This additional N-terminal truncation is also supported by the retention of the C-terminal His tag on examination by Western blotting analyses (data not shown). These results indicate that the signal sequence is absent in the purified sample. Approximately 30 mg pure protein was obtained per 12 l of culture. Two crystal forms (form I and form II) were obtained for the unlabelled protein, corresponding to the presence (form I) and absence (form II) of zinc in the reservoir solution. Form I crystals grew to average dimensions of 0.4 × 0.2 × 0.1 mm in one week (Fig. 3*a*) and the crystals started dissolving after one month (Fig. 3*b*). Therefore, we collected X-ray images within three weeks of crystallization setup. These crystals diffracted X-rays to a maximum of 7 Å resolution. Two cycles of annealing improved the diffraction limit from 7 Å resolution to approximately 3 Å resolution and the unit-cell parameters were reduced from $a = b = 124.9$, $c = 86.4$ Å to $a = b = 121.2$, $c = 83.9$ Å. These crystals belong to the tetragonal space group $P4_12_12$ or $P4_32_12$. Assuming the presence of two or three molecules in the asymmetric unit, the Matthews coefficient V_M was calculated to be 3.1 or 2.1 Å^3 Da^{-1}, respectively. No samarium sites were found in anomalous difference Patterson maps. Form II crystals reached average dimensions of 0.2 × 0.1 × 0.1 mm in one week and the crystals tended to be severely clustered (Fig. 3*c*). The obtained diffraction images were indexed and scaled to 3.0 Å resolution. Form II crystals belong to the monoclinic space group *C*2, with unit-cell parameters $a = 183.5$, $b = 47.2$, $c = 182.9$ Å, $\beta = 91.8°$. Assuming the presence of 5–10 molecules in the asymmetric unit, the corresponding V_M values were calculated to be 3.4–1.7 Å^3 Da^{-1} (Matthews, 1968). Crystallization of the selenomethionylated protein was performed under the same conditions as for the unlabelled protein. Although form I crystals of

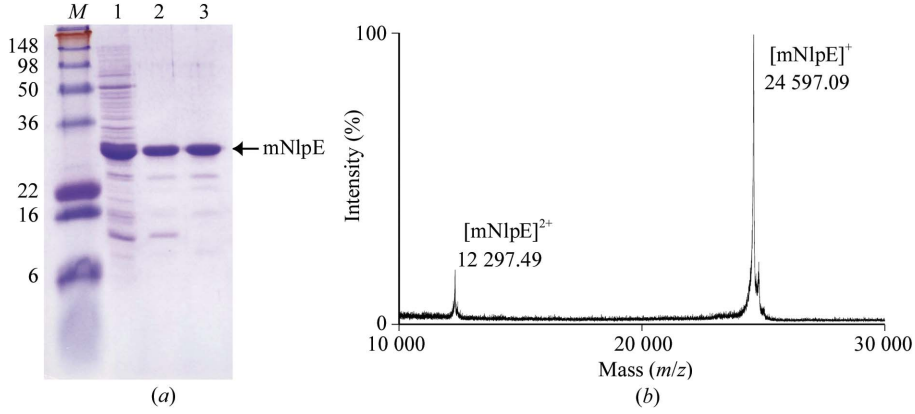

(*a*) (*b*)

Figure 2
(*a*) Each purification step of mNlpE from *E. coli* was analyzed by SDS–PAGE. Lane 1, periplasmic fraction from *E. coli* MC4100 cells; lane 2, 250 m*M* imidazole fraction from a TALON column; lane 3, peak fractions from an HA column; lane *M*, molecular-weight markers (kDa). (*b*) MALDI–MS spectrum of purfied mNlpE. The +1 and +2 charge states of mNlpE are indicated.

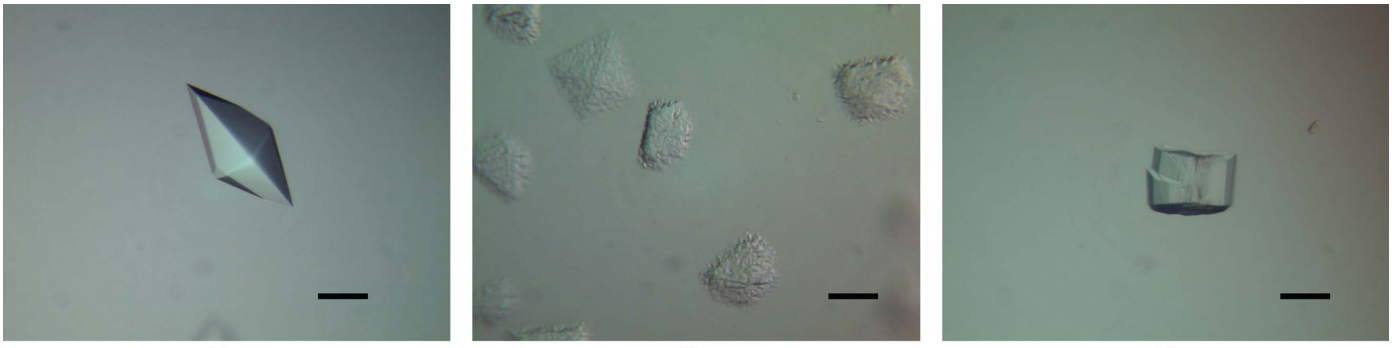

(*a*) (*b*) (*c*)

Figure 3
Crystals of the outer membrane lipoprotein mNlpE from *E. coli*. The black bars indicate 0.1 mm. (*a*) Tetragonal crystal (form I) of the unlabelled protein with approximate dimensions of 0.4 × 0.2 × 0.1 mm. (*b*) Tetragonal crystals (form I) of the selenomethionylated protein incubated for one month; the crystals showed a tendency to dissolve within one month. Crystals of the unlabelled proteins also tended to dissolve within two months. (*c*) Monoclinic crystal (form II) of the unlabelled protein with approximate dimensions of 0.2 × 0.1 × 0.1 mm.

Table 1
Data-collection statistics for the two crystal forms and for the form I crystal of the selenomethionyl-substituted protein.

Values in parentheses indicate statistics for the highest resolution shell.

	Unlabelled		SeMet MAD (form I)			
	Form I	Form II	High remote	Peak	Edge	Low remote
Space group	$P4_32_12$	$C2$	$P4_32_12$			
Unit-cell parameters (Å, °)	a = 121.2, b = 121.2, c = 83.9	a = 183.5, b = 47.2, c = 182.9, β = 91.8	a = 121.6, b = 121.6, c = 84.5			
Wavelength (Å)	1.6000	1.0000	0.9700	0.9792	0.9797	0.9900
Resolution range (Å)	40–2.8 (2.90–2.80)	50–3.0 (3.10–3.00)	50–3.1 (3.21–3.10)			
Observed reflections	119885	87996	101612	101865	99952	101191
Unique reflections	15130	29475	11615	11657	11529	11637
R_{sym}† (%)	8.1 (30.6)	7.3 (24.2)	11.7 (29.3)	12.1 (30.6)	11.3 (30.2)	11.1 (30.8)
$I/\sigma(I)$	22.6 (2.4)	15.6 (2.1)	16.7 (2.8)	16.4 (2.8)	16.0 (2.8)	16.2 (2.6)
Completeness (%)	95.0 (75.3)	92.4 (67.9)	96.7 (84.0)	96.4 (83.6)	96.0 (80.3)	95.7 (79.9)

† $R_{sym} = \sum_{hkl}\sum_i |I_{hkl,i} - \langle I_{hkl}\rangle| / \sum_{hkl}\sum_i I_{hkl,i}$, where $I_{hkl,i}$ is the ith measured diffraction intensity and $\langle I_{hkl}\rangle$ is the average of the intensity. Bijvoet pairs of the SeMet data were kept separate but scaled simultaneously and R_{sym} values were calculated with the Bijvoet pairs merged.

the selenomethionylated protein were obtained, form II crystals were never observed. The annealing method was also applied to form I crystals of the selenomethionylated protein in order to improve the diffraction limit. To prevent radiation damage while collecting the MAD data sets, the four data sets were collected with shorter exposure times than for the data sets of the unlabelled protein. Each data set was indexed and scaled to 3.1 Å resolution. The crystallographic statistics for all data sets are listed in Table 1. 13 of a possible 16 selenium sites for two NlpE molecules in the asymmetric unit were found using the anomalous signals from the peak-wavelength data. The experimental phases were calculated and refined at 4.0 Å resolution. The initial electron-density map was improved by solvent flipping and phase extension was performed to 3.1 Å resolution. The electron-density map calculated in space group $P4_32_12$ indicated a clear boundary between molecules and solvent and displayed some secondary-structure elements, whereas the map calculated in the alternative enantiomorph $P4_12_12$ was not interpretable. Consequently, we unambiguously concluded that the form I crystals belong to space group $P4_32_12$. The values of the overall figure of merit before and after density modification were 0.72 and 0.96, respectively.

We thank Drs T. Hikima, T. Matsu and M. Yamamoto for their help in data collection at SPring-8. This work was supported by grants for the National Project on Protein Structural and Functional Analyses from the Ministry of Education, Culture, Sports, Science and Technology.

References

Adachi, S., Oguchi, T., Tanida, H., Park, S.-Y., Shimizu, H., Miyatake, H., Kamiya, N., Shiro, Y., Inoue, Y., Ueki, T. & Iizuka, T. (2001). *Nucl. Instrum. Methods A*, **467–468**, 711–714.
Arnesano, F., Banci, L., Bertini, I., Mangani, S. & Thompsett, A. R. (2003). *Proc. Natl Acad. Sci. USA*, **100**, 3814–3819.
Brünger, A. T., Adams, P. D., Clore, G. M., DeLano, W. L., Gros, P., Grosse-Kunstleve, R. W., Jiang, J.-S., Kuszewski, J., Nilges, M., Pannu, N. S., Read, R. J., Rice, L. M., Simonson, T. & Warren, G. L. (1998). *Acta Cryst.* D**54**, 905–921.
Buelow, D. R. & Raivio, T. L. (2005). *J. Bacteriol.* **187**, 6622–6630.
Danese, P. N. & Silhavy, T. J. (1998). *J. Bacteriol.* **180**, 831–839.
Danese, P. N., Snyder, W. B., Cosma, C. L., Davis, L. J. & Silhavy, T. J. (1995). *Genes Dev.* **9**, 387–398.
Dartigalongue, C. & Raina, S. (1998). *EMBO J.* **17**, 3968–3980.
Duguay, A. R. & Silhavy, T. J. (2004). *Biochim. Biophys. Acta*, **1694**, 121–134.
Gupta, S. D., Lee, B. T., Camakaris, J. & Wu, H. C. (1995). *J. Bacteriol.* **177**, 4207–4215.
Isaac, D. D., Pinkner, J. S., Hultgren, S. J. & Silhavy, T. J. (2005). *Proc. Natl Acad. Sci. USA*, **102**, 17775–17779.
McRee, D. E. (1999). *J. Struct. Biol.* **125**, 156–165.
Mares, M., Meloun, B., Pavlik, M., Kostka, V. & Baudys, M. (1989). *FEBS Lett.* **251**, 94–98.
Masuda, K., Matsuyama, S. & Tokuda, H. (2002). *Proc. Natl Acad. Sci. USA*, **99**, 7390–7395.
Matsuyama, S., Tajima, T. & Tokuda, H. (1995). *EMBO J.* **14**, 3365–3372.
Matsuyama, S., Yokota, N. & Tokuda, H. (1997). *EMBO J.* **16**, 6947–6955.
Matthews, B. (1968). *J. Mol. Biol.* **33**, 491–497.
Miyadai, H., Tanaka-Masuda, K., Matsuyama, S. & Tokuda, H. (2004). *J. Biol. Chem.* **279**, 39807–39813.
Otto, K. & Silhavy, T. J. (2002). *Proc. Natl Acad. Sci. USA*, **99**, 2287–2292.
Otwinowski, Z. & Minor, W. (1997). *Methods Enzymol.* **276**, 307–326.
Pogliano, J., Lynch, A. S., Belin, D., Lin, E. C. & Beckwith, J. (1997). *Genes Dev.* **11**, 1169–1182.
Raffa, R. G. & Raivio, T. L. (2002). *Mol. Microbiol.* **45**, 1599–1611.
Raivio, T. L., Laird, M. W., Joly, J. C. & Silhavy, T. J. (2000). *Mol. Microbiol.* **37**, 1186–1197.
Raivio, T. L., Popkin, D. L. & Silhavy, T. J. (1999). *J. Bacteriol.* **181**, 5263–5272.
Ruiz, N. & Silhavy, T. J. (2005). *Curr. Opin. Microbiol.* **8**, 122–126.
Schneider, T. R. & Sheldrick, G. M. (2002). *Acta Cryst.* D**58**, 1772–1779.
Snyder, W. B., Davis, L. J. B., Danese, P. N., Cosma, C. L. & Silhavy, T. J. (1995). *J. Bacteriol.* **177**, 4216–4223.
Song, H. K. & Suh, S. W. (1998). *J. Mol. Biol.* **275**, 347–363.
Takeda, K., Miyatake, H., Yokota, N., Matsuyama, S., Tokuda, H. & Miki, K. (2003). *EMBO J.* **22**, 3199–3209.
Terada, M., Kuroda, T., Matsuyama, S. & Tokuda, H. (2001). *J. Biol. Chem.* **276**, 47690–47694.
Yakushi, T., Masuda, K., Narita, S., Matsuyama, S. & Tokuda, H. (2000). *Nature Cell Biol.* **2**, 212–218.
Yamaguchi, K., Yu, F. & Inouye, M. (1988). *Cell*, **53**, 423–432.
Yamamoto, K. & Ishihama, A. (2005). *Mol. Microbiol.* **56**, 215–227.
Yamamoto, K. & Ishihama, A. (2006). *Biosci. Biotechnol. Biochem.* **70**, 1688–1695.
Yeh, J. I. & Hol, W. G. (1998). *Acta Cryst.* D**54**, 479–480.